IEEE Access
Multidisciplinary ⋮ Rapid Review ⋮ Open Access Journal

Received 8 June 2024, accepted 30 June 2024, date of publication 4 July 2024, date of current version 16 July 2024.

Digital Object Identifier 10.1109/ACCESS.2024.3423722

RESEARCH ARTICLE

Sensor Fault Detection for LPV Systems Using Interval Observers

JORGE YUSEF COLÍN-CASTILLO[1], GLORIA LILIA OSORIO-GORDILLO[1], VICENÇ PUIG[2], RODOLFO AMALIO VARGAS-MÉNDEZ[1], GERARDO VICENTE GUERRERO-RAMÍREZ[1], (Senior Member, IEEE), JUAN REYES-REYES[1], AND CARLOS MANUEL ASTORGA-ZARAGOZA[1]

[1]Tecnológico Nacional de México/CENIDET, Interior Internado Palmira S/N, Cuernavaca, Morelos 62490, Mexico
[2]Institute of Robotics and Industrial Informatics Polytechnic, University of Catalonia C/Llorens i Artigas 4-6, 08028 Barcelona, Spain

Corresponding author: Gloria Lilia Osorio-Gordillo (gloria.og@cenidet.tecnm.mx)

ABSTRACT This paper presents an approach for design a continuous-time interval observer for linear parameter varying (LPV) systems in the presence of disturbances that are considered unknown but bounded. The proposed observer is used for the design of a sensor fault detection scheme using the input to state stability (ISS) approach through a Lyapunov quadratic function. The conditions of stability and positivity are presented by a set of linear matrix inequalities (LMIs). The performance of the proposed method is shown in simulation using a case study based on a single-link flexible joint robotic system.

INDEX TERMS Interval observer, fault detection, interval estimation, sensor fault, linear parameter varying system.

I. INTRODUCTION

Fault detection is the process of discovering in real-time the presence of a fault in an equipment before it causes a breakdown using the available sensors. This topic has gained special interest during the last decades in the industry and academia because of the growing complexity of equipment and components in industrial processes making them prone to the occurrence of faults. A fault in a process can degrade its performance, reduce component life, generate unscheduled shutdowns (which can result in economic losses) and can even lead to human losses. Actually, in the area of automatic control, one of the most used techniques for the development of fault detection schemes are the observers, which are used to obtain a simultaneous estimation of states and faults, as shown in [1], [2], [3], and [4]. In the same way, these approaches have also been used to design robust schemes such as fault tolerant controls as shown in [5]. In model-based approaches, there always exist modeling uncertainties that make difficult to estimate a variable when using observers with a minimum degree of robustness. A possible robust state estimation scheme relies on the concept of interval observers, where an interval of estimated states is obtained under the assumptions that the uncertainties are unknown but bounded.

Interval observers have received considerable attention in recent years. Different approaches have been proposed to deal with different class of continuous-time and discrete-time systems, such as [6], [7], and [8]. The main limitation of interval observers is that the trajectories of the system that start from an internally bounded initial condition will enclose the stable system trajectory only if the system is *positive* that is, the system matrix is Metzler and Hurwitz [9]. The positivity of the error estimation is one of the most restrictive assumptions for interval observer design. Recently, the concept of interval observer has been extended to switched classes, see as e.g. [10], [11], [12], where the idea is to apply a combination of time-varying similarity transformations along with the observer's gains, which guarantee both positivity and practical stability of the switched dynamics of the estimation errors, as proposed in [13], [14], and [15]. There are different approaches to perform fault detection scheme, in which are the classical observers, such as [16], [17], and [18] where they calculate an asymptotic estimation based on the inputs and outputs of the system. Similarly, the concept of interval

The associate editor coordinating the review of this manuscript and approving it for publication was Mauro Fadda.

observers has been applied to fault detection schemes, as it considers the limits of uncertainties to provide the bounds for estimating the system state, thus having an interval estimate. Being thus considered as a natural threshold for detection as shown in [19], [20], [21], [22], and [23]. The advantage of these two estimation strategies is that they are usually more computationally efficient, since they use observers with a single degree of freedom L. However, due to the simplicity of the observer, low magnitude of faults may be undetected. This means that the efficiency of the fault detection scheme is highly dependent on the observer degrees of freedom. For this reason, the *TNL* design strategy is proposed, which is based on adding additional degrees of freedom T and N in the observer design as described in [24] and [25].

This paper presents a methodology to design a fault detection scheme preserving the properties of the interval state estimation for linear parameter varying (LPV) systems. It outlines a Linear Matrix Inequalities (LMIs) approach to determine interval observers with positive observer gains using Metzler system matrix parametric constraints and the common quadratic function input to state stability (ISS) Lyapunov function to guarantee the stability to mitigate the effect of uncertainties on the residual signals. The performance of the proposed method is shown in simulation using a case study based on a single-link flexible joint robotic system.

The structure of the paper is the following: In Section II, introductory background materials regarding interval matrices and systems is provided. Section III introduces the problem statement. Section IV presents the interval observer design procedure. Section V illustrates the method with the proposed robotic case study and the application to fault detection. Section VI draws the main conclusions and present future research paths.

Notation: The symbol I_n denotes the identity matrix of dimension n. The symbol $(*)$ denotes the transposed part in a symmetric position. The matrices A^T denotes the transpose of the matrix $A \in \mathbb{R}^{n\times m}$, $A^\dagger$ is the Moore-Penrose inverse of matrix A. $A \succ 0$ denotes a real positive-definite matrix A ($A \succeq 0$, semidefinite positive), $A \prec 0$ denotes a real negative-definite matrix A ($A \preceq 0$, semidefinite negative). The Hermitian part of a square matrix A is denoted by $\mathcal{H}(A) = A + A^T$. The Euclidean norm of $x(t)$ is $||x(t)||_2 = x^T(t)x(t)$ and the $\mathcal{L}_\infty$ norm of $x(t)$ is $||x(t)||_\infty = \sup\{||x(t)||_2, t \in \mathbb{R}_+\}$.

II. PRELIMINARIES

Lemma 1: [26] Consider the following equation of a non homogeneous system

$$XA = B \tag{1}$$

where $A \in \mathbb{R}^{m\times p}$ and $B \in \mathbb{R}^{n\times p}$ are constant matrices, and $X \in \mathbb{R}^{n\times m}$ is the matrix to be determined.

The equation (1) admits a solution, if and only if

$$rank(A) = rank\begin{bmatrix} A \\ B \end{bmatrix}$$

in this case, the general solution to equation (1) is given by:

$$X = BA^\dagger - Y(I - AA^\dagger)$$

where Y is an arbitrary matrix of appropriate dimension.

A. INTERVAL ANALYSIS

Consider a matrix A that can be decomposed as $A = A^+ - A^-$, where $A^+ = \max\{0, A\}$ (the maximum operator is understood elementwise) and A^- can be computed as $A^- = A^+ - A$, such that $A^+ \geq 0$ and $A^- \geq 0$. The above operations can be extended to any vector $x \in \mathbb{R}^n$.

Lemma 2: [27] Let $x(t) \in \mathbb{R}^n$ be a vector bounded by an interval $\overline{x}(t)$, $\underline{x}(t) \in \mathbb{R}^n$ such that $\underline{x}(t) \leq x(t) \leq \overline{x}(t)$.

1) *Let $A \in \mathbb{R}^{m\times n}$ be a constant matrix, such that $A = A^+ - A^-$, so then:*

$$A^+\underline{x}(t) - A^-\overline{x}(t) \leq Ax(t) \leq A^+\overline{x}(t) - A^-\underline{x}(t)$$

2) *Let A, $\underline{A}$, $\overline{A} \in \mathbb{R}^{m\times n}$ be matrices such that $\underline{A} \leq A \leq \overline{A}$. Then:*

$$\underline{A}^+\underline{x}^+ - \overline{A}^+\underline{x}^- - \underline{A}^-\overline{x}^+ + \overline{A}^-\overline{x}^- \leq Ax \leq \overline{A}^+\overline{x}^+ - \underline{A}^+\overline{x}^- - \overline{A}^-\underline{x}^+ + \underline{A}^-\underline{x}^-$$

Definition 1: [28] A matrix $A = [a_{ij}] \in \mathbb{R}^{n\times n}$ is called Metzler if all its off-diagonal elements are nonnegative, i.e. $a_{ij} \geq 0$, $i \neq j$. The Metzler condition prevents the generation of the wrapping effect within the interval estimates.

Lemma 3: [29] The matrix A is Metzler if there exists an scalar $\eta > 0$ such that $A + \eta I_n \geq 0$.

III. PROBLEM STATEMENT

A. PROBLEM SET-UP

Consider a continuous-time polytopic LPV system

$$\begin{aligned} \dot{x}(t) &= \sum_{i=1}^{k} \mu_i(\rho(t))(A_i x(t) + B_i u(t)) + Ew(t), \\ y(t) &= Cx(t) + Ff(t), \end{aligned} \tag{2}$$

where $x(t) \in \mathbb{R}^n$ is the state vector, $u(t) \in \mathbb{R}^q$ is the vector of system inputs, $y(t) \in \mathbb{R}^p$ represents the measured output, $w(t) \in \mathbb{R}^r$ is an exogenous input considered as disturbance, and $f(t) \in \mathbb{R}^s$ is a sensor fault. $\rho(t) = \{\rho_1(t), \ldots, \rho_m(t)\}$ is a vector of varying parameters that embed the nonlinearities of the system. Furthermore assume that $\rho(t)$ is available (i.e. perfectly measurable) for the observer which will be proposed. $F \in \mathbb{R}^{p\times s}$ is the fault distribution matrix, $E \in \mathbb{R}^{n\times r}$ is the disturbance distribution matrix, $A_i \in \mathbb{R}^{n\times n}$, $B_i \in \mathbb{R}^{n\times q}$ and $C \in \mathbb{R}^{p\times n}$ are known matrices of appropriate dimensions.

$\mu_i(\rho(t))$ are the weighting functions of each i^{th} vertex model. This functions must satisfy the following restrictions:

$$0 \leq \mu_i(\rho(t)) \leq 1, \quad \sum_{i=1}^{k} \mu_i(\rho(t)) = 1 \tag{3}$$

where $k = 2^m$ is the number linear vertex models, and m are the number of varying parameters.

Assumption 1: The disturbance vector $w(t)$ is considered unknown but with known bounds as follows:

$$\underline{w}(t) \leq w(t) \leq \overline{w}(t). \tag{4}$$

Assumption 2: The initial state vector $x(0)$ satisfies

$$\underline{x}(0) \leq x(0) \leq \overline{x}(0), \tag{5}$$

where $\underline{x}(0)$, $\overline{x}(0) \in \mathbb{R}^n$ are constant vectors.

Lemma 4: Let $E \in \mathbb{R}^{n\times r}$ be a constant matrix and $w(t) \in \mathbb{R}^r$, considering Lemma 2 and Assumption 1, we obtain

$$E^+\underline{w}(t) - E^-\overline{w}(t) \leq Ew(t) \leq E^+\overline{w}(t) - E^-\underline{w}(t). \tag{6}$$

For the continuous-time LPV system (2), the following interval observer proposed is:

$$\dot{\overline{\zeta}}(t) = \sum_{i=1}^{k} \mu_i(\rho(t))((TA_i - L_iC)\overline{\hat{x}}(t) + TB_iu(t) + L_iy(t)) + \bigtriangleup, \tag{7}$$

$$\overline{\hat{x}}(t) = \overline{\zeta}(t) + Ny(t), \tag{8}$$

$$\overline{\hat{y}}(t) = C\overline{\hat{x}}(t), \tag{9}$$

$$\dot{\underline{\zeta}}(t) = \sum_{i=1}^{k} \mu_i(\rho(t))((TA_i - L_iC)\underline{\hat{x}}(t) + TB_iu(t) + L_iy(t)) + \bigtriangledown, \tag{10}$$

$$\underline{\hat{x}}(t) = \underline{\zeta}(t) + Ny(t), \tag{11}$$

$$\underline{\hat{y}}(t) = C\underline{\hat{x}}(t), \tag{12}$$

where $\overline{\zeta}(t) \in \mathbb{R}^n$ and $\underline{\zeta}(t) \in \mathbb{R}^n$ represent auxiliary interval vectors, the vectors $\overline{\hat{x}}(t) \in \mathbb{R}^n$ and $\underline{\hat{x}}(t) \in \mathbb{R}^n$ represent the upper and lower estimates of the state vector $x(t)$, and $\overline{\hat{y}}(t) \in \mathbb{R}^p$ and $\underline{\hat{y}}(t) \in \mathbb{R}^p$ are the upper and lower estimates of the measured output $y(t)$. L_i, T and N are gain matrices to be designed. Matrices $\bigtriangleup$ and $\bigtriangledown$ are defined as follows:

$$\bigtriangleup = (TE)^+\overline{w}(t) - (TE)^-\underline{w}(t), \tag{13}$$

$$\bigtriangledown = (TE)^+\underline{w}(t) - (TE)^-\overline{w}(t). \tag{14}$$

Passive fault detection strategy is a technique that allows the detection of faults in a system by comparing the measured output $y(t) \in \mathbb{R}^p$ and the estimated one $\hat{y}(t) \in \mathbb{R}^p$. This comparison is based on generating a residual signal

$$r(t) = \hat{y}(t) - y(t). \tag{15}$$

Assumption 3: The fault detection scheme proposed in this paper considers $f(t) = 0$ for the observer design, such that the output $y(t)$ of the system (2) is expressed as $y(t) = Cx(t)$.

From Lemma 2, the following expressions can be obtained for equations (9) and (12), respectively

$$\overline{\hat{y}}(t) = C^+\overline{\hat{x}}(t) - C^-\underline{\hat{x}}(t), \tag{16}$$

$$\underline{\hat{y}}(t) = C^+\underline{\hat{x}}(t) - C^-\overline{\hat{x}}(t). \tag{17}$$

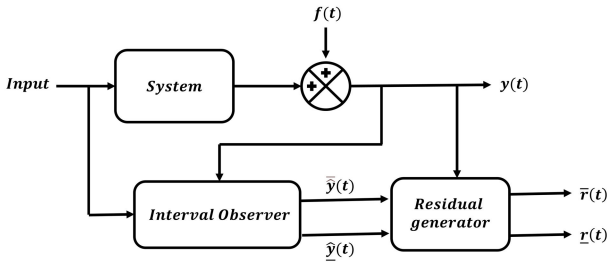

FIGURE 1. Fault detection scheme based on interval observer.

In the bounded disturbance context, it is possible to detect a fault by constructing the following residual signal bounds (see Figure 1)

$$\overline{r}(t) = \overline{\hat{y}}(t) - y(t), \tag{18}$$

$$\underline{r}(t) = \underline{\hat{y}}(t) - y(t). \tag{19}$$

So, in case $0 \in [\overline{r}(t), \underline{r}(t)]$ no fault can be indicated. Otherwise, if $1 \notin [\overline{r}(t), \underline{r}(t)]$ a fault is detected. This strategy is efficient to avoid false alarms that occur due to the presence of disturbances in the system. However, it is possible that low magnitude faults may not be detected because of the disturbance bounds described in Assumption 1.

B. OBSERVER DESIGN

The objective of the interval observer design (7-12) is to estimate an upper and lower bound of the state vector $x(t)$, which allows enclosing the set of admissible values of the system state (2) while ensuring the convergence of the estimation errors.

From Assumption 3, the dynamics of both estimation error bounds are given by

$$\overline{e}(t) = \overline{\hat{x}}(t) - x(t), \tag{20}$$

$$\underline{e}(t) = x(t) - \underline{\hat{x}}(t), \tag{21}$$

by replacing (8) into (20), we obtain

$$\overline{e}(t) = \overline{\zeta}(t) - Tx(t), \tag{22}$$

where

$$T = NC - I_n, \tag{23}$$

in a similar manner, it follows from (21)

$$\underline{e}(t) = Tx(t) - \underline{\zeta}(t). \tag{24}$$

The dynamic evolution of the error (22) is

$$\dot{\overline{e}}(t) = \dot{\overline{\zeta}}(t) - T\dot{x}(t), \tag{25}$$

$$= \sum_{i=1}^{k} \mu_i(\rho(t))(TA_i - L_iC)\overline{e}(t) + (TE)^+\overline{w}(t) - (TE)^-\underline{w}(t) - TEw(t), \tag{26}$$

and from (24)

$$\dot{\underline{e}}(t) = T\dot{x}(t) - \dot{\underline{\zeta}}(t), \tag{27}$$

$$= \sum_{i=1}^{k} \mu_i(\rho(t))(TA_i - L_iC)\underline{e}(t) + TEw(t) - (TE)^{+}\underline{w}(t) + (TE)^{-}\overline{w}(t). \tag{28}$$

According to Lemma 2 and Assumption 1, the following inequalities are obtained

$$(TE)^{+}\overline{w}(t) - (TE)^{-}\underline{w}(t) - TEw(t) \geq 0,$$
$$TEw(t) - (TE)^{+}\underline{w}(t) + (TE)^{-}\overline{w}(t) \geq 0. \tag{29}$$

Considering that the stability of the interval LPV observer results from the stability of the interval error we get

$$e(t) = \overline{\hat{x}}(t) - \underline{\hat{x}}(t), \tag{30}$$
$$= \overline{e}(t) + \underline{e}(t), \tag{31}$$

the dynamics of the interval error is obtained as follows

$$\dot{e}(t) = \dot{\overline{e}}(t) + \dot{\underline{e}}(t), \tag{32}$$
$$= \sum_{i=1}^{k} \mu_i(\rho(t))\Big[(TA_i - L_iC)e(t) + M\omega(t)\Big], \tag{33}$$

where $M = \begin{bmatrix} (TE)^{+} & -(TE)^{-} \end{bmatrix}$, $\omega(t) = \begin{bmatrix} \overline{w}(t) - \underline{w}(t) \\ \underline{w}(t) - \overline{w}(t) \end{bmatrix}$.

According to (29), the matrices $(TA_i - L_iC)$ satisfy the Metzler condition. Thus, taking into account initial conditions $\underline{e}(0) = x(0) - \underline{\hat{x}}(0), \overline{e}(0) = \overline{\hat{x}}(0) - x(0)$, the interval observer will provide a positive estimate, which will ensure the correct interval state bounds.

Considering the bounded term of the perturbation $\omega(t)$ from Assumption 1, the objective of the interval observer is to obtain the intervals for the error dynamics (33).

From equations (7-12) that define the interval observer, the estimation errors $\overline{e}(t)$ and $\underline{e}(t)$ must be stable by means of the ISS function. The ISS function allows to guarantee the observer stability and attenuate the effect of disturbances on the interval estimates of $x(t)$.

C. PARAMETERIZATION OF THE OBSERVER

Considering that equation (23) can be written as

$$\begin{bmatrix} T & N \end{bmatrix} \Sigma = I_n, \tag{34}$$

where $\Sigma = \begin{bmatrix} I_n \\ C \end{bmatrix}$, and since $rank(\Sigma) = n$ the general solution of (34) is given by

$$T = \underbrace{\Sigma^{\dagger}\begin{bmatrix} I_n \\ 0 \end{bmatrix}}_{T_1} + Z \underbrace{(I_{n+p} - \Sigma\Sigma^{\dagger})\begin{bmatrix} I_n \\ 0 \end{bmatrix}}_{T_2}, \tag{35}$$

$$N = \underbrace{\Sigma^{\dagger}\begin{bmatrix} 0 \\ I_p \end{bmatrix}}_{N_1} + Z \underbrace{(I_{n+p} - \Sigma\Sigma^{\dagger})\begin{bmatrix} 0 \\ I_p \end{bmatrix}}_{N_2}, \tag{36}$$

where $Z \in \mathbb{R}^{n\times(n+p)}$ is a matrix with arbitrary elements.

From the definition of the matrix T in equation (35), the dynamic of the interval estimation error (33) is represented as

$$\dot{e}(t) = \sum_{i=1}^{k} \mu_i(\rho(t))[\mathcal{A}_i e(t) + M\omega(t)], \tag{37}$$

where M and $\omega(t)$ are defined in (33), $\mathcal{A}_i = T_1A_i + ZT_2A_i - L_iC$.

Thus, the design of the observer is reduced to determine matrix L_i, such that (37) is stable. The value of the Z matrix is a design parameter of the proposed interval observer. For simplicity, it is considered to be known.

IV. INTERVAL OBSERVER DESIGN PROCEDURE

In this section, a method to design the interval observer (7-12) is presented. Sufficient ISS conditions are given to guarantee the stability and positivity of the dynamic error (33) to obtain matrix L_i.

Theorem 1: For the LPV system (2) with $f(t) = 0$, there exists a Lyapunov function $V(e(t)) = e^T(t)Pe(t)$, if there exist a positive diagonal matrix P, matrix R_i, scalars $\beta > \alpha > 0$, $\gamma > 0$ for a given $\epsilon \geq 1$, $\alpha \geq 1$ and $\eta > 0$, such that the following LMIs are satisfied

$$\min_{P,\, R_i,\, \gamma}$$
$$\alpha I_n \preceq P \preceq \beta I_n, \tag{38}$$
$$\begin{bmatrix} \mathcal{H}(PT_1A_i + PZT_2A_i - R_iC) + \epsilon P & (*) \\ \begin{bmatrix} (P(TE)^{+})^T \\ (-P(TE)^{-})^T \end{bmatrix} & -\gamma I_n \end{bmatrix} \preceq 0, \tag{39}$$
$$PT_1A_i + PZT_2A_i - R_iC + \eta P \geq 0, \tag{40}$$

then the system (7-12) can asymptotically estimate the lower and upper bounds of the state vector $x(t)$.

Proof 1: Consider the following quadratic ordinary ISS-Lyapunov function

$$V(e(t)) = e^T(t)Pe(t) \succ 0, \tag{41}$$

where $P \in \mathbb{R}^{n\times n}$ is a positive diagonal matrix.

The derivative of (41) along the trajectory of (37) gives

$$\dot{V}(e(t)) = \dot{e}^T(t)Pe(t) + e^T(t)P\dot{e}(t), \tag{42}$$
$$= \sum_{i=1}^{k} \mu_i(\rho(t))\Big[e^T(t)\big(\mathcal{A}_i^T P + P\mathcal{A}_i\big)e(t)\Big] + e^T(t)PM\omega(t) + \omega^T(t)M^T Pe(t) \prec 0. \tag{43}$$

Let $\varsigma(t) = \begin{bmatrix} e(t) \\ \omega(t) \end{bmatrix}$, then we obtain the following inequality

$$\dot{V}(e(t)) + \epsilon V(e(t)) - \gamma\omega^T(t)\omega(t) \leq \varsigma^T(t)\Omega\varsigma(t), \tag{44}$$

with

$$\Omega = \begin{bmatrix} \mathcal{A}_i P + P\mathcal{A}_i + \epsilon P & PM \\ M^T P & -\gamma I_n \end{bmatrix},$$

where ϵ *and* γ *are positive scalars. Replacing* $\mathcal{A}_i$ *and* M *from (37) we obtain*

$$\Omega = \begin{bmatrix} \mathcal{H}(PT_1A_i + PZT_2A_i - R_iC) + \epsilon P & (*) \\ \begin{bmatrix} (P(TE)^+)^T \\ (-P(TE)^-)^T \end{bmatrix} & -\gamma I_n \end{bmatrix}, \quad (45)$$

where $R_i = PL_i$ *is an unknown matrix of appropriate dimensions.*

According to [11], the system (37) is ISS if $\Omega \preceq 0$ *since* $\omega^T(t)\omega(t) < \infty$ *leading to*

$$\dot{V}(e(t)) \leq \varsigma^T(t)\Omega\varsigma(t) - \epsilon V(e(t)) + \gamma\omega^T(t)\omega(t), \quad (46)$$

so that, the term in the right side of this inequality is negative.

Therefore, the following inequality is satisfied:

$$\dot{V}(e(t)) \leq -\epsilon V(e(t)) + \gamma\omega^T(t)\omega(t). \quad (47)$$

By integrating the two sides of this inequality, we obtain

$$V(e(t)) \leq e^{-\epsilon t}V(0) + \gamma\int_0^\infty e^{-\epsilon(t-s)}||\omega(s)||_2\, ds, \quad (48)$$

knowing that (41) is satisfied for some scalar $\beta > \alpha > 0$*, the following inequality is proposed*

$$\alpha||e(t)||_2^2 \leq V(e(t)) \leq \beta||e(t)||_2^2, \quad (49)$$

which allows to deduce

$$||e(t)||_2 \leq \frac{1}{\sqrt{\alpha}}\left(e^{-\epsilon t}V(0) + \frac{\gamma}{\epsilon}||\omega(t)||_\infty\right)^{1/2}. \quad (50)$$

Hence, when $t \to \infty$ *the exponential converge to zero, which implies that*

$$\lim_{t\to\infty}||e(t)||_2 \leq \sqrt{\frac{\gamma}{\alpha\epsilon}}\max||\omega(t)||_\infty. \quad (51)$$

Note that using the ISS concept the boundness of the interval error is guaranteed. Consequently, the design of an interval observer with a tight interval may be achieved optimally, if the bound $\sqrt{\frac{\gamma}{\alpha\epsilon}}\max||\omega(t)||_\infty$ *is minimized. Therefore, the problem of minimizing the upper bound of the interval error is reduced to the minimization of the scalar* γ *for a given* $\alpha \geq 1$ *and* $\epsilon \geq 1$.

In a second step, we need to ensure $\mathcal{A}_i$ *Metzler. From Lemma 3,* $\mathcal{A}_i$ *is Metzler if there exists an scalar* $\eta > 0$ *such that*:

$$\mathcal{A}_i + \eta I \geq 0. \quad (52)$$

Since only the off-diagonal elements of $\mathcal{A}_i$ *must be nonnegative to satify the Metzler property, the term* ηI *is added as shown in (52). By pre-multiplying the inequality (52) by a positive diagonal matrix P from (41), the matrix* $P\mathcal{A}_i$ *is also Metzler yielding to*

$$PT_1A_i + PZT_2A_i - R_iC + \eta P \geq 0, \quad (53)$$

which proves the positivity of the interval errors for a positive definite diagonal matrix P. Thus, we conclude that the state vector is always bounded by the solutions of the interval observer.

V. APPLICATION TO THE CASE STUDY

To illustrate the performance of the proposed observer (7-12), the model of a one-link flexible joint robot driven by a DC motor system is used (see Figure 2).

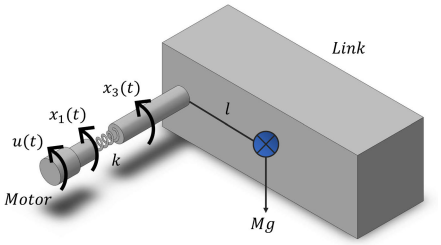

FIGURE 2. One-link-flexible joint robot.

The mathematical model of a one-link flexible-joint robot is given by

$$\begin{aligned} \dot{x}_1(t) &= x_2(t), \\ \dot{x}_2(t) &= -\frac{b_V x_2(t)}{J} - \frac{k(x_1(t) - x_3(t))}{J} + \frac{k_\tau}{J}(u(t)), \\ \dot{x}_3(t) &= x_4(t), \\ \dot{x}_4(t) &= -\frac{Mglsen(x_3(t))}{I} - \frac{k(x_3(t) - x_1(t))}{I}, \\ y(t) &= \begin{bmatrix} x_1(t) \\ x_2(t) \\ x_3(t) \end{bmatrix}, \end{aligned} \quad (54)$$

where $x_1(t)$ is the angular rotation of the motor (rad), the angular velocity of the motor is $x_2(t)$ (rad/s), $x_3(t)$ is the angular rotation of the link (rad), $x_4(t)$ is the angular velocity of the link (rad/s), $u(t)$ is the supply voltage to the motor (V) and $y(t)$ are the measured outputs of the system. The parameter descriptions and values are presented in Table 1.

TABLE 1. Parameter definition and values.

Parameter	Value	Definition
g	9.81 m/s^2	Gravity
M	0.31 Kg	Link Mass
l	0.15 m	Link Mass Center
k	0.18 Nm/rad	Elasticity coefficient
b_v	0.0083 Nms/rad	Coefficient of viscous friction
K_τ	0.08 Nm/V	Amplification gain
J	0.0037 Kgm^2	Motor inertia
I	0.0093 Kgm^2	Inertia of the link

A. LPV MODEL REPRESENTATION

The model (54) contains a nonlinearity $sen(x_3(t))$. These equations can be represented by following LPV

representation

$$\dot{x}(t) = A(x(t))x(t) + Bu(t) + Ew(t),$$
$$y(t) = Cx(t) + Ff(t), \tag{55}$$

where $w(t)$ represents the distribution of a uniform noise in an interval $[-0.2, 0.2]$, $f(t)$ represents sensor faults, matrices E and F are distribution matrices.

From (55) the matrices of the system are defined as

$$A(x(t)) = \begin{bmatrix} 0 & 1 & 0 & 0 \\ -\frac{k}{J} & -\frac{b_V}{J} & \frac{k}{J} & 0 \\ 0 & 0 & 0 & 1 \\ \frac{k}{I} & 0 & \rho(t) & 0 \end{bmatrix}, \quad E = \begin{bmatrix} 0 \\ 0 \\ 1 \\ 1 \end{bmatrix}, B = \begin{bmatrix} 0 \\ \frac{k_\tau}{J} \\ 0 \\ 0 \end{bmatrix},$$

$F = \begin{bmatrix} 1 \\ 0 \\ 1 \end{bmatrix}$ and $C = \begin{bmatrix} 1 & 0 & 0 & 0 \\ 0 & 1 & 0 & 0 \\ 0 & 0 & 1 & 0 \end{bmatrix}$, where $\rho(t)$ represents a grouping of the nonlinear term as

$$\rho(t) = -\frac{k}{I} - \frac{Mgl}{I}\frac{sen(x_3(t))}{x_3(t)}. \tag{56}$$

The weighting functions are defined as:

$$\mu_1(\rho(t)) = \frac{\overline{\rho} - \rho(t)}{\overline{\rho} - \underline{\rho}}, \ \mu_2(\rho(t)) = \frac{\rho(t) - \underline{\rho}}{\overline{\rho} - \underline{\rho}}, \tag{57}$$

where $\overline{\rho}$ and $\underline{\rho}$ are the known upper and lower limit of $\rho(t)$, respectively.

The system (54) can be expressed in the polytopic form as:

$$\dot{x}(t) = \sum_{i=1}^{2} \mu_i(\rho(t))(A_i x(t)) + Bu(t) + Ew(t),$$
$$y(t) = Cx(t) + Ff(t), \tag{58}$$

where $A_1 = \begin{bmatrix} 0 & 1 & 0 & 0 \\ -48.64 & -1.25 & 48.6 & 0 \\ 0 & 0 & 0 & 1 \\ 19.35 & 0 & \underline{\rho} & 0 \end{bmatrix}$,

$A_2 = \begin{bmatrix} 0 & 1 & 0 & 0 \\ -48.64 & -1.25 & 48.6 & 0 \\ 0 & 0 & 0 & 1 \\ 19.35 & 0 & \overline{\rho} & 0 \end{bmatrix}, B = \begin{bmatrix} 0 \\ 21.62 \\ 0 \\ 0 \end{bmatrix}$,

the matrices E, F and C were defined in (55).

B. SIMULATION RESULTS

By considering an input $u(t) = 1V$ and a variation of the noise inside the interval $[-0.2, 0.2]$, the limits of variation of $\rho(t)$ are $\underline{\rho} = -70$, $\overline{\rho} = -66.30$.

Consider a constant input $u(t) = 1V$, noise variation is presented in Figure 3 which implies that $\overline{w}(t) = w(t) + 0.1$, $\underline{w}(t) = w(t) - 0.1$.

The system is simulated taking into account the following initial conditions $x(0) = \begin{bmatrix} 0.5 & 0 & 0.5 & 0 \end{bmatrix}^T$, and for the observer $\overline{\hat{x}}(0) = \begin{bmatrix} 1 & 1 & 1 & 1 \end{bmatrix}^T$, $\underline{\hat{x}}(0) = \begin{bmatrix} -1 & -1 & -1 & -1 \end{bmatrix}^T$.

The selected parameters are $\eta = 10$, $\epsilon = 1$, $\alpha = 1$, $\beta = 5$ and solving the optimization problem of Theorem 1 with a minimization factor of $\gamma = 2.18$ using Matlab software

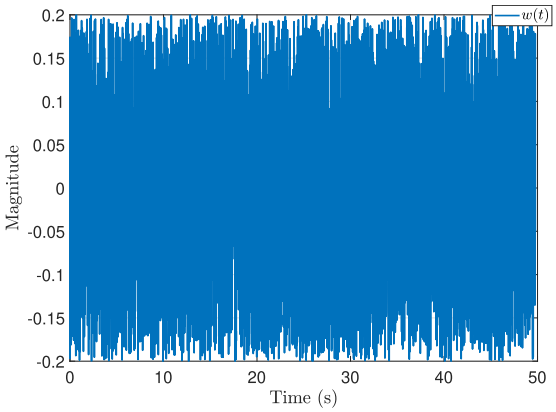

FIGURE 3. Noise signal.

and the YALMIP-SeDuMi toolbox, we obtain the following interval observer gains described by

$$L_1 = \begin{bmatrix} 10 & -1.1893 & -6.3398 \times 10^{-10} \\ -24.3243 & 7.1891 & 24.3243 \\ -6.3251 \times 10^{-10} & -1.1893 & 10 \\ 19.3548 & 4.7279 & -70 \end{bmatrix},$$

$$L_2 = \begin{bmatrix} 10 & -1.1893 & -6.3384 \times 10^{-10} \\ -24.3243 & 7.1891 & 24.3243 \\ -6.3236 \times 10^{-10} & -1.1893 & 10 \\ 19.3548 & 4.7279 & -66.300 \end{bmatrix},$$

$$T = \begin{bmatrix} -1.1893 & 0 & 1.1893 & 0 \\ -1.6893 & 0.50 & 1.1893 & 0 \\ -1.1893 & 0 & 1.1893 & 0 \\ 4.7279 & 0 & -5.7279 & 1 \end{bmatrix},$$

$$N = \begin{bmatrix} 2.1893 & 0 & -1.1893 \\ 1.6893 & 0.50 & -1.1893 \\ 1.1893 & 0 & -0.1893 \\ -4.7279 & 0 & 5.7279 \end{bmatrix},$$

$$Z = \begin{bmatrix} -3.3786 & 0 & 2.3786 & 0 & 0 & 0 & 0 \\ -3.3786 & 0 & 2.37863 & 0 & 0 & 0 & 0 \\ -2.3786 & 0 & 1.3786 & 0 & 0 & 0 & 0 \\ 9.4557 & 0 & -11.4557 & 0 & 0 & 0 & 0 \end{bmatrix} \text{ and } P = I_4.$$

The first scenario considers the outputs without the presence of fault. Figure 4 shows the estimation of the system outputs (the black line represents the nonlinear behavior of the state, the blue and red line represent the lower and upper interval estimate, respectively). Figure 5 shows that the upper and lower residuals remain close to zero, this means that no fault has been detected.

To evaluate the performance of the fault detection approach, two scenarios are proposed.

The sensor fault signal of the first scenario is

$$f(t) = \begin{cases} 0.1 & 5 \leq t \leq 10 \\ -0.2 & 25 \leq t \leq 35 \\ 0 & otherwise \end{cases} \tag{59}$$

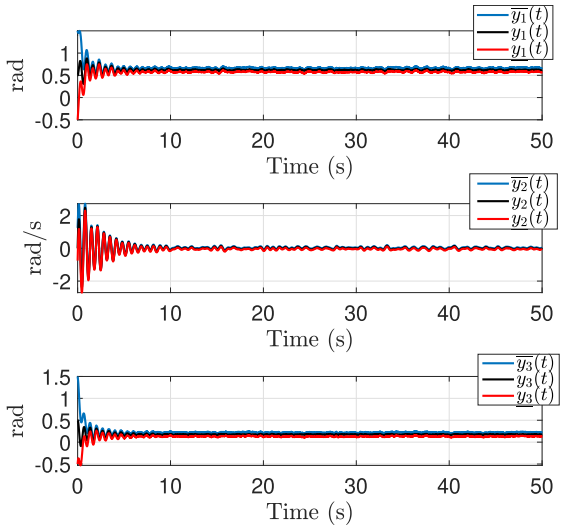

FIGURE 4. Measured output and output estimation without fault.

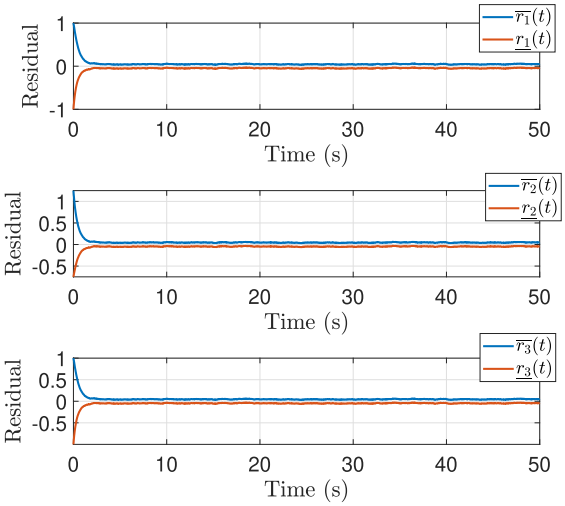

FIGURE 5. Upper residuals and lower residuals without fault.

which represents a fault due to overheating in the motor windings, which generates an abrupt increase in the input magnitude.

The simulation results are shown in Figures 6 - 9. When the fault described in the equation (59) occurs, there are changes in the output and residual intervals. So, in case $0 \in [\overline{r}(t), \underline{r}(t)]$ no fault can be indicated, otherwise, if $1 \notin [\overline{r}(t), \underline{r}(t)]$ a fault is detected.

The Figure 6 shows that at $t = 5$ and $t = 10$, the upper $\overline{y}(t)$ and lower $\underline{y}(t)$ intervals of $y(t)$ do not generate an adequate signal envelope, due to the presence of the fault. The same behavior is presented at time $t = 25$ and $t = 35$.

The Figures 7 - 9 shows that the residuals are no longer at the observer's natural threshold, this due to the presence of fault in the output signals. The table 2 shows a fault signature matrix obtained from the analysis of symptoms.

TABLE 2. Fault signature matrix of the first scenario.

	Abrupt fault		
Residual	$5 \leq t \leq 10$	$25 \leq t \leq 35$	**otherwise**
r_1	1	1	0
r_2	1	1	0
r_3	1	1	0

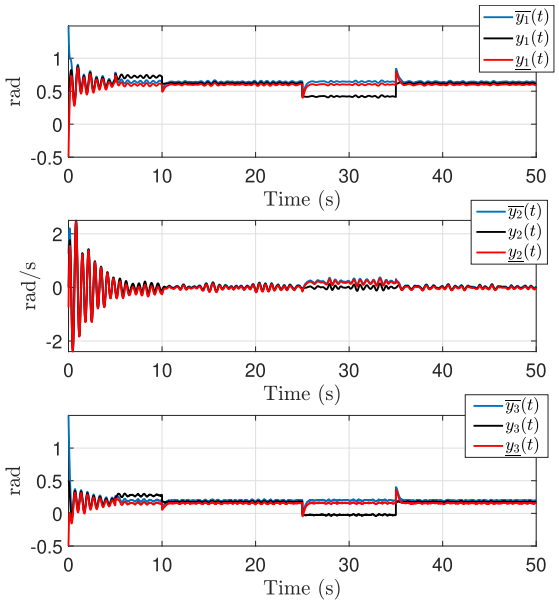

FIGURE 6. Measured output and output estimation with abrupt fault.

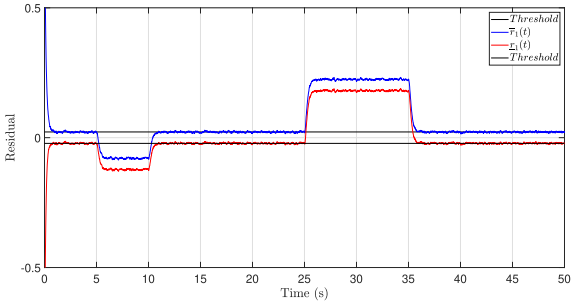

FIGURE 7. Residual r_1 upper and lower with abrupt fault.

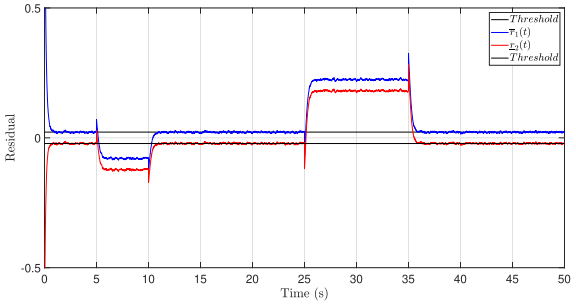

FIGURE 8. Residual r_2 upper and lower with abrupt fault.

A second scenario is proposed, considering the following time-varying sensor fault

$$f(t) = \begin{cases} 0.01 & 15 \leq t \leq 20 \\ 0.01 + t & 20 \leq t \leq 35 \\ 0 & otherwise \end{cases} \quad (60)$$

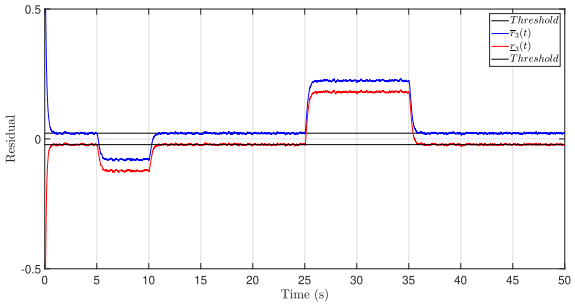

FIGURE 9. Residual r_3 upper and lower with abrupt fault.

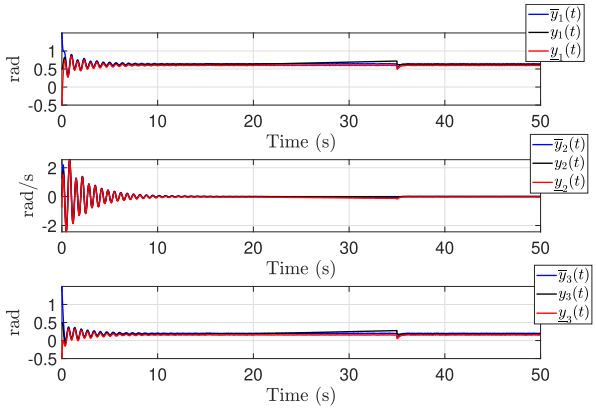

FIGURE 10. Measured output and output estimation with incipient fault.

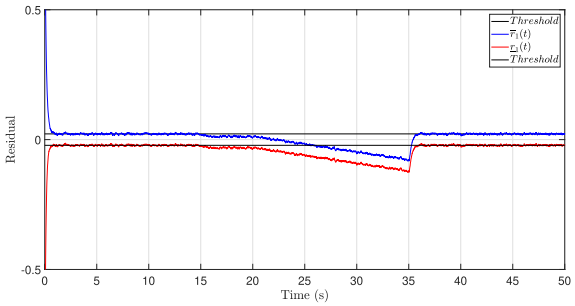

FIGURE 11. Residual r_1 upper and lower with incipient fault.

which represents a bad calibration in the angular position sensors.

The simulation results of the second scenario are shown in Figures 10 - 13. When the fault described in the equation (60) occurs, there are changes in the output and residual intervals.

The Figure 10 shows that at $t = 15$ and $t = 20$, the upper $\overline{y}(t)$ and lower $\underline{y}(t)$ intervals of $y(t)$ do not perform an adequate envelopment due to the presence of fault. When the fault becomes incipient in the time $t = 20$ and $t = 35$, it can be seen that the output variables present an increasing behavior until they get away from the interval estimates.

The Figures 11 - 13 shows that the residuals are no longer at the observer's natural threshold, this due to the presence of fault in the output signals.

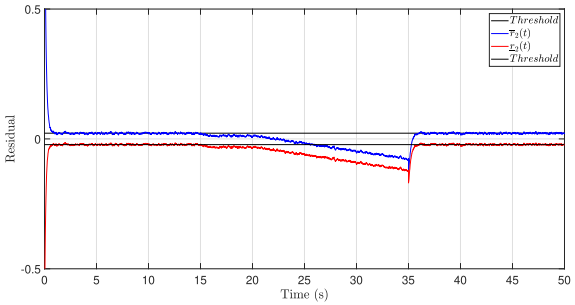

FIGURE 12. Residual r_2 upper and lower with incipient fault.

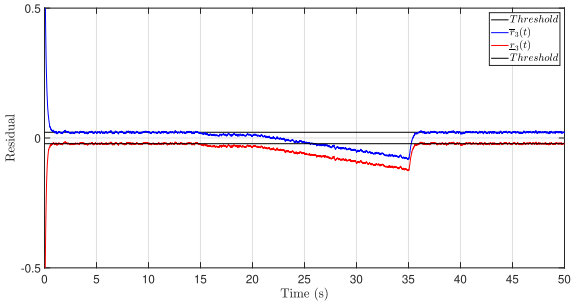

FIGURE 13. Residual r_3 upper and lower with incipient fault.

TABLE 3. Fault signature matrix of the second scenario.

	Incipient fault		
Residual	$15 \leq t \leq 20$	$20 \leq t \leq 35$	**otherwise**
r_1	1	1	0
r_2	1	1	0
r_3	1	1	0

The Table 3 shows a fault signature matrix for comparison of the classical scheme with respect to the interval scheme.

VI. CONCLUSION

This paper has presented the design of a robust fault detection scheme for continuous-time LPV systems which are subject to disturbances which are considered unknown but bounded. The fault detection scheme is composed of an observer that perform robust estimation of the system outputs with their respective intervals. An advantage of this type of interval schemes is the generation of a natural threshold generated by the shares of exogenous inputs that affect the system, such as noise or parametric variations. The results show that the fault detection scheme enforces robustness when generating a residual response againts the bounded disturbances that are present in system (2). The stability criteria based on the ISS approach is proposed to adjust the observer gains. At the same time, this approach allows mitigating the effect of the unknown disturbance. To validate the efficiency of the fault detection scheme, the model of a flexibly articulated robot has been used providing satisfactory results. As future research, the proposed approach will extended to fault isolation and estimation.

REFERENCES

[1] R. Aguilar, J. González, J. Alvarez-Ramirez, and M. A. Barrón, "Temperature regulation of a class of continuous chemical reactor based on a nonlinear Luenberger-like observer," *J. Chem. Technol. Biotechnol.*, vol. 70, no. 3, pp. 209–216, Nov. 1997.

[2] F. Celani, "A Luenberger-style observer for robot manipulators with position measurements," in *Proc. 14th Medit. Conf. Control Autom.*, Dec. 2006, pp. 1–6.

[3] H. Hamdi, M. Rodrigues, C. Mechmeche, D. Theilliol, and N. B. Braiek, "State estimation for polytopic LPV descriptor systems: Application to fault diagnosis," *IFAC Proc. Volumes*, vol. 42, no. 8, pp. 438–443, 2009.

[4] J. Han, X. Liu, X. Wei, and X. Hu, "Adaptive adjustable dimension observer based fault estimation for switched fuzzy systems with unmeasurable premise variables," *Fuzzy Sets Syst.*, vol. 452, pp. 149–167, Jan. 2023.

[5] J. Han, X. Liu, X. Xie, and X. Wei, "Dynamic output feedback fault tolerant control for switched fuzzy systems with fast time varying and unbounded faults," *IEEE Trans. Fuzzy Syst.*, vol. 31, no. 9, pp. 3185–3196, Sep. 2023.

[6] D. Efimov, L. Fridman, T. Raïssi, A. Zolghadri, and R. Seydou, "Interval estimation for LPV systems applying high order sliding mode techniques," *Automatica*, vol. 48, no. 9, pp. 2365–2371, Sep. 2012.

[7] J. Blesa, D. Rotondo, V. Puig, and F. Nejjari, "FDI and FTC of wind turbines using the interval observer approach and virtual actuators/sensors," *Control Eng. Pract.*, vol. 24, pp. 138–155, Mar. 2014.

[8] L. Meyer, D. Ichalal, and V. Vigneron, "Interval observer for bilinear systems with unknown inputs," in *Proc. Annu. Amer. Control Conf. (ACC)*, Jun. 2018, pp. 5957–5961.

[9] L. Farina and S. Rinaldi, *Positive Linear Systems: Theory and Applications*. Hoboken, NJ, USA: Wiley, 2000.

[10] S. Guo and F. Zhu, "Interval observer design for discrete-time switched system," *IFAC-Papers OnLine*, vol. 50, pp. 5073–5078, Jul. 2017.

[11] S. Ifqir, V. Puig, D. Ichalal, N. Ait-Oufroukh, and S. Mammar, "Set-membership switched observers based on interval characterization of the estimation error," *IFAC-PapersOnLine*, vol. 53, no. 2, pp. 14261–14266, 2020.

[12] Q. Su, Z. Fan, T. Lu, Y. Long, and J. Li, "Fault detection for switched systems with all modes unstable based on interval observer," *Inf. Sci.*, vol. 517, pp. 167–182, May 2020.

[13] T. N. Dinh, G. Marouani, T. Raïssi, Z. Wang, and H. Messaoud, "Optimal interval observers for discrete-time linear switched systems," *Int. J. Control*, vol. 93, no. 11, pp. 2613–2621, Nov. 2020.

[14] D. Li, J. Chang, W. Chen, and T. Raïssi, "IPR-based distributed interval observers design for uncertain LTI systems," *ISA Trans.*, vol. 121, pp. 147–155, Feb. 2022.

[15] Z. Huang, "Application of interval state estimation in vehicle control," *Alexandria Eng. J.*, vol. 61, no. 1, pp. 911–916, Jan. 2022.

[16] F. Caccavale and I. D. Walker, "Observer-based fault detection for robot manipulators," in *Proc. Int. Conf. Robot. Autom.*, Apr. 1997, pp. 2881–2887.

[17] M. A. Eissa, M. S. Ahmed, R. R. Darwish, and A. M. Bassiuny, "Improved fuzzy Luenberger observer-based fault detection for BLDC motor," in *Proc. 10th Int. Conf. Comput. Eng. Syst. (ICCES)*, Dec. 2015, pp. 167–174.

[18] H. Jeong, B. Park, S. Park, H. Min, and S. Lee, "Fault detection and identification method using observer-based residuals," *Rel. Eng. Syst. Saf.*, vol. 184, pp. 27–40, Apr. 2019.

[19] J. Meseguer, V. Puig, and T. Escobet, "Fault diagnosis using a timed discrete-event approach based on interval observers: Application to sewer networks," *IEEE Trans. Syst. Man, Cybern. A, Syst. Humans*, vol. 40, no. 5, pp. 900–916, Sep. 2010.

[20] R. Lamouchi, M. Amairi, T. Raissi, and M. Aoun, "Interval observer design for linear parameter-varying systems subject to component faults," in *Proc. 24th Medit. Conf. Control Autom. (MED)*, Jun. 2016, pp. 707–712.

[21] C. Zhang, X. Wang, and Y. Ren, "Actuator fault detection for autonomous underwater vehicle using interval observer," in *Proc. CAA Symp. Fault Detection, Supervision Saf. Tech. Processes (SAFEPROCESS)*, Jul. 2019, pp. 449–453.

[22] Z.-H. Zhang and G.-H. Yang, "Distributed fault detection and isolation for multiagent systems: An interval observer approach," *IEEE Trans. Syst. Man, Cybern. Syst.*, vol. 50, no. 6, pp. 2220–2230, Jun. 2020.

[23] F. Zhu, Y. Tang, and Z. Wang, "Interval-observer-based fault detection and isolation design for T-S fuzzy system based on zonotope analysis," *IEEE Trans. Fuzzy Syst.*, vol. 30, no. 4, pp. 945–955, Apr. 2022.

[24] Z. Wang, C.-C. Lim, and Y. Shen, "Interval observer design for uncertain discrete-time linear systems," *Syst. Control Lett.*, vol. 116, pp. 41–46, Jun. 2018.

[25] M. Hou, H. Shi, G. Oancea, and X. Bai, "Fault detection based on modified interval observer for discrete-time linear system," *Manuf. Eng.*, vol. 18, no. 4, pp. 1–8, 2020.

[26] D. Bernstein, *Matrix Mathematics: Theory, Facts, and Formulas*, 2nd ed., Princeton, NJ, USA: Princeton Univ. Press, 2008.

[27] D. Efimov, T. Raissi, and A. Zolghadri, "Control of nonlinear and LPV systems: Interval observer-based framework," *IEEE Trans. Autom. Control*, vol. 58, no. 3, pp. 773–778, Mar. 2013.

[28] H. Thomas, *The Mathematics of Frobenius in Context: A Journey Through 18th to 20th Century Mathematics*. New York, NY, USA: Springer, 2013.

[29] M. A. Rami and F. Tadeo, "Positive observation problem for linear discrete positive systems," in *Proc. 45th IEEE Conf. Decis. Control*, Dec. 2006, pp. 4729–4733.

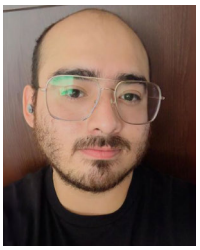

JORGE YUSEF COLÍN-CASTILLO received the bachelor's degree in mechatronics engineering from Universidad del Valle de México, Cuernavaca, Morelos, Mexico, in 2018, and the M.Sc. degree in electronic engineering in the area of automatic control from the National Center for Research and Technological Development, CENIDET, Mexico, in 2020. He is currently pursuing the Ph.D. degree in automatic control with CENIDET. His research interests include the design of interval observers for Takagi-Sugeno systems, LPV, fault diagnosis, and fault tolerant control.

GLORIA LILIA OSORIO-GORDILLO received the M.Sc. degree from the Centro Nacional de Investigación y Desarrollo Tecnológico (CENIDET), in 2011, and the double Ph.D. degree in automatic control from the University of Lorraine, France, and TECNM/CENIDET, Mexico, in 2015. She has been with CENIDET, as a Research Professor, since 2015. Her research interests include observers design for descriptor, Takagi-Sugeno, LPV systems, fault diagnosis, and fault tolerant control.

VICENÇ PUIG received the dual B.S./M.S. degree in telecommunications engineering and the Ph.D. degree in automatic control, robotics and computer vision from the Universitat Politècnica de Catalunya (UPC), Barcelona, Spain, in 1993 and 1999, respectively. He is currently a Full Professor with the Automatic Control Department, UPC, and a Researcher with the Institute of Robotics and Industrial Informatics (IRI), CSIC-UPC. He has made important contributions in the areas of fault diagnosis and fault tolerant control, using interval and linear-parameter-varying models.

RODOLFO AMALIO VARGAS-MÉNDEZ received the M.Sc. degree in electronic engineering from the Centro Nacional de Investigación y Desarrollo Tecnológico (CENIDET), Mexico, in 2011, and the Ph.D. degree in electronics engineering in the area of power electronics from CENIDET, in 2015. He has been with CENIDET, as a Research Professor, since 2016. His research interests include multilevel inverters symmetric and asymmetric topologies, carrier-based PWM methods, space-vector modulation, and fault-tolerant systems.

GERARDO VICENTE GUERRERO-RAMÍREZ (Senior Member, IEEE) received the B.Sc. degree in electrical engineering from the Technological Institute of Morelia, Mexico, in 1985, the M.Sc. degree in electronic engineering from the Centro Nacional de Investigación y Desarrollo Tecnológico (TecNM/CENIDET), Cuernavaca, Mexico, in 1994, and the Ph.D. degree in engineering from the Universidad Nacional Autónoma de México (UNAM), in 2001. He is currently a full-time Professor with the Automatic Control Group, Electronic Engineering Department, CENIDET, where he has involved in modeling and control of systems based on energetic approaches and other related topics, such as AC motor control and fault diagnosis topics.

JUAN REYES-REYES received the M.Sc. and Ph.D. degrees from the Advanced Research and Studies Center (CINVESTAV), Mexico, in 1997 and 2001, respectively. He has Level 1 membership grade with the National Researchers System, Mexico. He is currently a Research Professor with TecNM/Cenidet, Cuernavaca, Mexico. His research interests include control of uncertain nonlinear systems, dynamic neural networks, Lyapunov analysis, sustainable, and biologically inspired systems.

CARLOS MANUEL ASTORGA-ZARAGOZA received the Ph.D. degree in process engineering from the Université Claude Bernard Lyon 1, France, in 2001. Since 1993, he has been holding teaching and research positions with the Tecnológico Nacional de México/CENIDET. His research interests include observers and fault detection systems for energy conversion processes.